Int. J. Nav. Archit. Ocean Eng. (2015) 7:70~86
http:// dx.doi.org/10.2478/IJNAOE-2015-0006
pISSN: 2092-6782, eISSN: 2092-6790

Inner harbour wave agitation using boussinesq wave model

Jitendra K. Panigrahi[1], C.P. Padhy[2] and A.S.N. Murty[1]

[1]*Department of Marine Sciences, Berhampur University, Berhampur, India*
[2]*Department of Ocean Engineering & Naval Architecture, Indian Institute of Technology, Kharagpur, India*

ABSTRACT: *Short crested waves play an important role for planning and design of harbours. In this context a numerical simulation is carried out to evaluate wave tranquility inside a real harbour located in east coast of India. The annual offshore wave climate proximity to harbour site is established using Wave Model (WAM) hindcast wave data. The deep water waves are transformed to harbour front using a Near Shore spectral Wave model (NSW). A directional analysis is carried out to determine the probable incident wave directions towards the harbour. Most critical threshold wave height and wave period is chosen for normal operating conditions using exceedence probability analysis. Irregular random waves from various directions are generated confirming to Pierson Moskowitz spectrum at 20m water depth. Wave incident into inner harbor through harbor entrance is performed using Boussinesq Wave model (BW). Wave disturbance experienced inside the harbour and at various berths are analysed. The paper discusses the progresses took place in short wave modeling and it demonstrates application of wave climate for the evaluation of harbor tranquility using various types of wave models.*

KEY WORDS: Boussinesq wave model; Harbour tranquility; Wave disturbance; Wave climate.

INTRODUCTION

The function of a harbour is to provide safe anchorage for vessels and to facilitate smooth transfer of cargo between ships and adjoined land. Assured harbour tranquillity is not only essential for safe anchorage, but it is also important for efficient port operation. Essentially, harbour tranquillity reduces to the excitation of ships moored at anchorage or along a wharf and optimises the mooring forces. Larger ships may not experience wave agitation to the wind-waves, whereas a small boat may be violently swung by the same wave. Thus, harbour tranquillity needs to be judged from the viewpoint of wave climate at ship's berthing areas. In the viewpoint of port operation, the relationship between ship motion and cargo handling works as well falls in the judgement of harbour tranquillity. Hence establishing statistics of the wave climate outside the harbour and transforming it to inner harbour berth locations is a fundamental task. In coastal engineering practice, the behavior of short waves in shallow water has long been concerned. For the design of harbors, a detailed knowledge is required for the direction of propagation and magnitude of short waves. These waves attack moles, training works, breakwaters and other structures, they infiltrate through harbour entrances to disturb the waters within the harbour area, both directly and through accumulated, seiching actions, they are instrumented in bringing sediments into suspension while they often induce the currents that transport these sediments to quieter regions of deposition, and they may also adversely influence navigation directly. As a result of the practical interest in these waves, a considerable research effort has gone to predict their behavior along coasts and in and around harbors, terminals

Corresponding author: *Jitendra K. Panigrahi*, e-mail: *Jitu@scientist.com*

and other engineering works. By far the greatest part of this effort has been directed towards developing the techniques for physical modelling and a veritable arsenal has been accumulated for this purpose like field and laboratory instrumentation, wave generators with their associated data processing, control and evaluation equipment and a wide range of analytical procedures. In the past efforts expended in numerical modeling by producing several useful techniques (Abbott et al., 1978a). Today, the advancement in this direction to an extent replaced the physical modeling.

In this study, numerical simulations are carried out for a real harbour (Fig. 1) at Gangavaram adjoining to Bay of Bengal, East Coast of India to evaluate the wave tranquillity condition for the master plan of harbour layout. The wave agitation levels at the harbour vicinity are modeled using approximately a decades (1995-2004) offshore wave data. Offshore wave data obtained from wave model 'WAM' (WAMDI Group, 1988) are analysed and transformed to nearshore. The wave disturbances in the harbour basin and berth locations are assessed using Boussinesq Wave Model (Abbott et al., 1978b). This study on penetration of offshore wave climate in to a harbour is a demonstration of application of wave climate for decision support to port planning. In Indian context, this study is a useful reference for port planners to resolve the decisions viz. allocation of berths for various types of vessels, width of the harbour entrance, configuration of breakwaters etc.

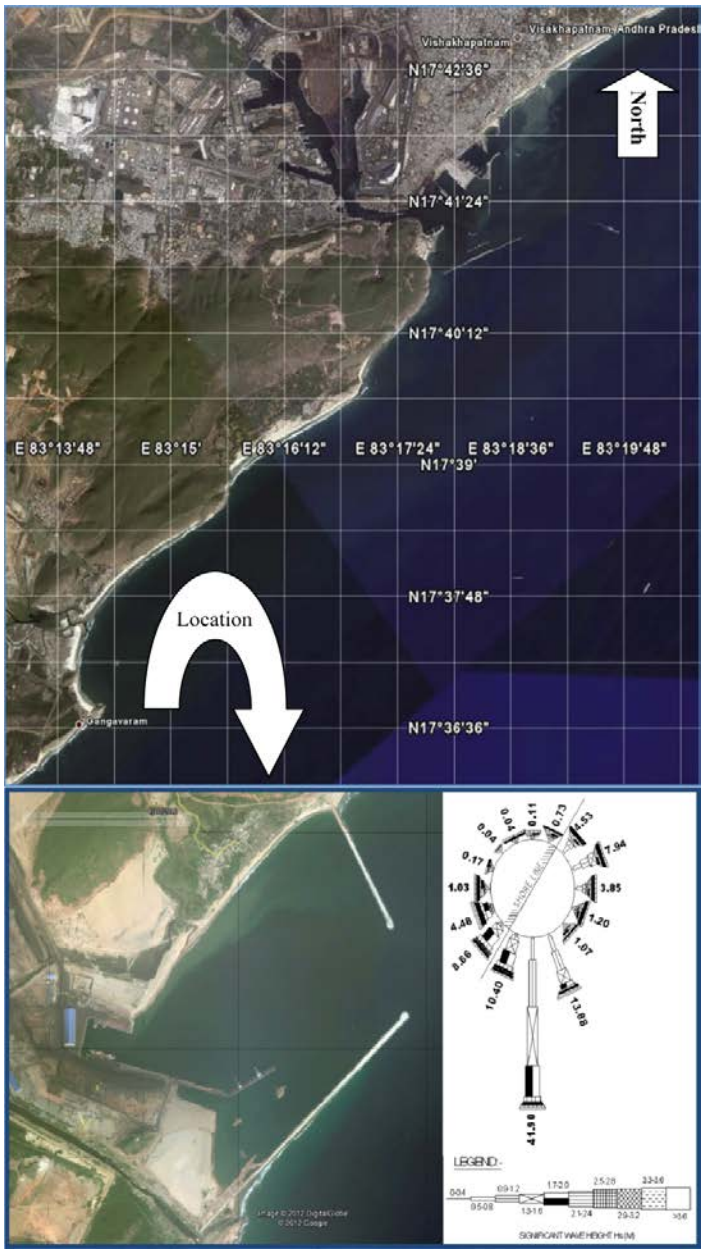

Fig. 1 Harbour Location and offshore wave rose.

REVIEW OF SHORT WAVE MODELING

The progress in wave modeling has contributed substantially to port planners in optimizing the harbor layouts. The present stage of 'short wave model' has evolved fast in past two decades. In order to relate the present simulation experiment using the latest short wave model with the earlier works, the review of wave theories provide a firm basis. The terminology of 'short crested waves' is that of common engineering practice. In classical hydrodynamics, however, what are here called short shallow water waves are viewed as waves whose length is still large compared with the depth of the water in which they propagate and they are correspondingly, usually subsumed under long waves. The various theories constructed to describe the behaviour of these waves are generally characterized by an Ursell number i.e. (Eq. (1)):

$$U_* = \frac{\zeta_* L_*^2}{h_*^3} \tag{1}$$

where ζ_* is a measure of the wave amplitude, L_* is a characteristic horizontal length of the surface profile and h_* is a measure of the water depth (Ursell, 1953). The earliest relevant theory, of Airy (Airy, 1845), makes the assumption that the pressure distribution in the vertical water column is hydrostatic. The resulting waves are non-dispersive, while waves of finite amplitude cannot propagate without change of shape. Airy`s theory corresponds to $U_* >> 0$ (1). The symmetric case of $U_* << 0$ (1) is covered by the linearised shallow water theory, which also assumes a hydrostatic pressure distribution. Between the theories of Airy (Airy, 1845) and Jeffreys (Jeffreys and Jeffreys, 2007) there is the theory of Boussinesq (Boussinesq, 1872; 1877). In this theory the curvature of streamlines in the vertical plane is described through a vertical velocity the magnitude of which increases linearly from zero at the bed to a maximum at the free surface. Therefore, the pressure distribution is no longer hydrostatic, but the vertical component of motion can be integrated out of the equations of motion to reduce the three dimensional description to a two-dimensional one. The original theory held for the irrotational motion of an incompressible, homogeneous, inviscid fluid over a horizontal bed, while only solutions for uni-directional wave propagation were considered. Ursell (1953) showed that the Boussinesq theory included the Airy and Jeffreys theories as special cases. Later, the Boussinesq theory was in fact be regarded as the most uniformly valid basis for finite amplitude water waves so long as h_*/L_* remains small and breaking does not occur. When $U_* = 0(1)$ the non-linear, governing equations for a horizontal bottom are of the Korteweg-De Vries (Korteweg and De Vries, 1895) type, that have unidirectional cnoidal waves as permanent solutions. Mei and Le Mehaute (Mei and Le Mehaute, 1966) extended solutions of the Boussinesq theory to include diffracted and reflected plane waves over a slowly varying bathymetry (Madsen and Mei, 1969). In 1967, Peregrine (Peregrine, 1967) derived the Boussinesq type equations governing the propagation of arbitrary, long-wave disturbances of small to moderate amplitude over a slowly-varying bathymetry. Subsequently, the system-generated models developed and are based upon Boussinesq equations, in which the vertical velocity was supposed to increase linearly from zero at the bed to a maximum magnitude at the surface, in two independent (horizontal) space variables and time. The Boussinesq equations are formulated as mass and momentum conservation laws while, by virtue of the high order of accuracy of the difference approximations, there is very little numerical energy falsification. This formulation also appears to provide genuine weak solutions, for correctly simulating breaking waves, and thus assures the correct simulation of wave thrusts, or radiation stresses, and associated longshore currents. In 1991 Madsen P.A (Madsen et al., 1991) introduced a new form of the Boussinesq equations, which improved the dispersion characteristics. It is demonstrated that the depth-limitation of the new equations is much less restrictive than for the classical forms of the Boussinesq equations, and it became possible to simulate the propagation of irregular wave trains travelling from deep water to shallow water. In deep water, the new equations become effectively linear and phase celerities agree with Stokes first-order theory. In more shallow water, the new equations converge towards the standard Boussinesq equations, which are known to provide good results for waves up to at least 75% of their breaking height. Also a numerical method for solving the new set of equations in two horizontal dimensions are introduced based on a time-centered implicit finite-difference scheme. Further a linear shoaling analysis of the new equations and a verification of the numerical model with respect to shoaling and refraction-diffraction in deep and shallow water are generalized. In nineties the model evolved to two-dimensional form of equations of the Boussinesq type (Madsen et al., 1997a; 1997b). It's features improved linear dispersion characteristics, possibility of wave breaking, and a moving boundary at the shoreline. The moving shoreline is treated numerically by replacing the solid beach by a permeable beach characterized by an extremely small porosity. The inclusion of wave breaking is based on the surface roller concept for spilling breakers using

a geometrical determination of the instantaneous roller thickness at each point and modelling the effect of wave breaking by an additional convective momentum term. This is a function of the local wave celerity, which is determined interactively. The model is applied to cross-shore motions of regular waves including various types of breaking on plane sloping beaches and over submerged bars. Model results comprise of time series surface elevations and the spatial variation of phase-averaged quantities such as the wave height, the crest and trough elevations, the mean water level, and the depth-averaged undertow. At present form of two-dimensional Boussinesq wave model, (Pierson and Moskowitz, 1964) the model equations are discretised in space using unstructured finite element technique. The standard Galerkin method with mixed interpolation are introduced. The time discretisation is performed using a predictor-corrector method (a 4th-order Adams-Bashforth-Moulton method). Currently, there are many forms of Boussinesq wave models available to user community, such as COULWAVE (Patrick and Philip, 2004), FUNWAVE (James et al., 1998), BOUSS-2D (Zeki Demirbilek and Okey, 2007) and BW Mike21 (Abott et al., 2001). In the present study the authors have used an accurate wave model BW, Mike-21 (Abott et al., 1984; Madsen and Sørensen, 1992) for demonstrating a real world application. The Boussinesq wave model is compared against physical models and field experiments (Kuang-ming, et al., 1987; Kofoed-Hansen et al., 2003) and has been proven that the model is reliable. It can provide a cost-efficient tool for prediction of waves in large coastal areas, which includes the surf zone and coastal structures (Sørensen et al., 1998).

OFFSHORE WAVE CLIMATE

The statistics of the offshore wave climate is very essential information outside the harbour for all water front planning. It can only be obtained either by instrumental wave measurement or by wave hindcasting. In Indian context, for a long time, synoptic coverage of wind data over an area of interest was a limitation for wave simulation. Furthermore, measured waves provide point data, are often sparse, and not available when and where desired. Surface winds over global oceans are critical for driving numerical sea state prediction models. Hence, use of analyzed wind fields (Lorenc, 1986; Kamineni et al., 2002) assimilating to third generation wave models is the only solution for deriving long term wave conditions. In the present study, wave conditions are based on 10 years (1995-2004) six hourly model hindcasts using deep water wave model WAM (WAMDI Group, 1988). The deep water wave is simulated over regional grid system of north Indian Ocean using climatological wind fields (Swain, 1997; Panigrahi, 2007). The details about the wind assimilation, modeling and validation of outputs are not presented here and can be referred from author's publication (Panigrahi and Swain, 2010; Swain et al., 2003). However a short description of WAM model physics is presented in following paragraphs.

The wave hindcast has been carried out using a state-of-the-art third generation wave model WAM (Cycle 4) originally developed by WAMDI Group, 1988. It incorporates latest physics and integrates the basic transport equation without any prior assumption on the shape of the wave spectrum (Gunther et al., 1992). Currently, it is being used for global and regional wave forecasting purposes by several institutions in the world. The model requires the wind input at the prescribed model grids and computes the evolution of two dimensional wave spectrum for the full set of degrees of freedom (Komen, 1996). The source terms and the basic transport equations are integrated for the prescribed time steps which includes both depth and current refraction. The model is being updated with new advances and continually validated with long-term measurements of moored buoys and satellite data.

The model is formulated in spherical coordinates and it solves the energy balance equation for two dimensional wave spectrum F (f, θ, λ, φ, t), which is a function of frequency f, direction θ, longitude λ, latitude φ and time t through integration of the basic transport equation (Eq. (2)),

$$\frac{\partial F}{\partial T}+\frac{\partial}{\partial \varphi}\left(\dot{\varphi}\, F\right)+\frac{\partial}{\partial \lambda}\left(\dot{\lambda}\, F\right)+\frac{\partial}{\partial \theta}\left(\dot{\theta}\, F\right)=S \tag{2}$$

where $\dot{\varphi}$, $\dot{\lambda}$ and $\dot{\theta}$ are the rates of changes of position and propagation direction of wave packets travelling along the great circle path as in Eqs. (3) - (5).

$$\dot{\varphi}=\frac{d\varphi}{dt}=v\, R^{-1}Cos\theta \tag{3}$$

$$\dot{\lambda} = \frac{d\lambda}{dt} = v\, Sin\theta \left(R\, Cos\varphi\right)^{-1} \tag{4}$$

$$\dot{\theta} = \frac{d\theta}{dt} = v\, Sin\theta\, Tan\varphi\, R^{-1} \tag{5}$$

where v = g/4πf denotes the group velocity, g is acceleration due to gravity and R is the radius of the earth.

The time and space evolution of ocean surface wave field or the source function S may be represented by (Eq. (6))

$$\frac{\partial F}{\partial t} + v \bullet \nabla F = \quad S \quad = S_{in} + S_{nl} + S_{ds} \tag{6}$$

where v = v (f, θ) is the deep water group velocity and the net source function S is represented as the sum of the input S_{in} by the wind, the non-linear transfer S_{nl} by resonant wave-wave interactions and dissipation S_{ds}. The advantage of this model is that, it exactly computes the evolution of two-dimensional directional wave spectrum including the spectral variance of non-linear wave–wave interaction. Also it takes care the extreme wind-wave conditions (Komen, 1996).

The source term for wind input is given in Eq. (7):

$$S_{in} \quad = \quad \gamma \,.\, F \tag{7}$$

where γ is the growth rate of the waves and is a function of friction velocity, wave direction, wind direction, the phase speed of the waves and the roughness length.

The dissipation term is represented as Eq. (8):

$$S_{dis} \quad = \quad \gamma_d \,.\, F \tag{8}$$

γ_d is the proportionality constant for dissipation of waves, the exact form of which is given in WAMDI Group (1988).

The wave model is capable of predicting the ocean wave spectrum. The spectrum has been decomposed into 25 frequency bins and 12 directional bins. The 25 frequencies of the model range from 0.042 *Hz* to 0.41 *Hz* on a logarithmic scale with $\Delta f / f = 0.1$, and the direction bins are at 30º resolution. In the present study, significant wave height computed using this spectrum has been used for the analysis. The spatial resolution of the wave model used in this study is 1.5º × 1.5º with three hourly time step of input wind (Panigrahi, 2007). The regional grid system of the wave model is catered as per the grid size of the input analysed wind fields. The model runs were made with surface wind analysis for the Indian Ocean covering the region bound by longitudes 30º E to 120º E and latitudes -30º to 30º N (Panigrahi and Swain, 2010).

Time series wave parameters are extracted at an offshore location approximately 75 *km* away from the proposed harbour location. A wave rose is prepared for resultant waves (higher of seas or swells) and the directional analysis is presented in Fig. 1. It is observed from the wave rose that, offshore waves predominantly approach to the study area from NE (4.53%), ENE (7.94%), E (3.85%), ESE (1.20%), SE (1.07%), SSE (13.88%), S (41.90%) and SSW (10.40%) respectively. An exceedence probability analysis is carried out to selected deep-water wave directions and presented in the Fig. 2. The analysis reveals that at deep-water, wave height exceeding 1.4 *m* (Hs) prevails approximately 52.17 days in a year. Further it is seen from the 10-years resultant wave data set, an upper limit of the wave period (Tm) range 7 *sec*. predominantly falls at wave height (Hs) class of 1.4 *m*. From this analysis it can be assumed that a combination of (Hs = 1.4 *m* and Tm = 7 *sec*.) is very critical threshold for evaluating wave tranquility inside the harbor during normal operating conditions. It is seen from the wave rose with respect to shoreline orientation that, the planned harbour breakwaters (Fig. 1) would give sheltering to the predominant waves from SSW and SW directions. However to examine the wave energy reaching to shallow water a near shore wave transformation is carried out in subsequent section.

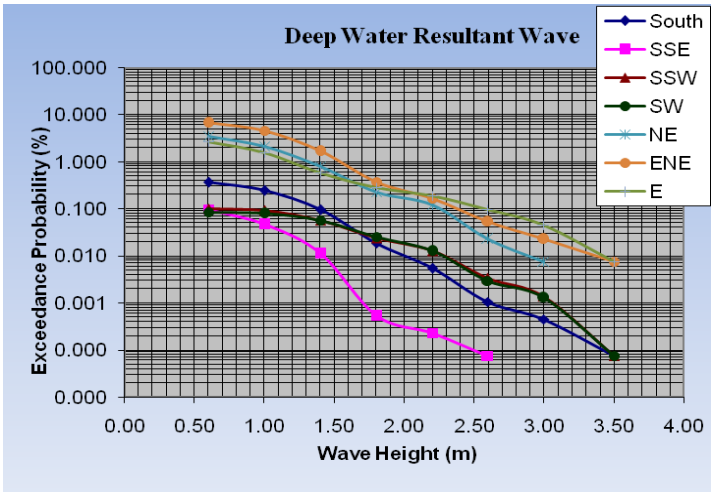

Fig. 2 Exceedence probability of offshore wave height.

NEARSHORE WAVE TRANSFORMATION

The deep water waves are transformed to shallow water using Nearshore Spectral Wind-wave (NSW) Model of DHI (Holthhuijsen, 1998). NSW is a stationary, directionally decoupled, parametric model which describes the propagation and decay of short period and short crested waves in nearshore areas. The model takes into account the effects of refraction, shoaling due to varying depth and dissipation due to bottom friction & wave breaking. The basic transport equation in the model is derived from the conservation equation for the spectral wave action density.

$$\frac{\partial(C_{gx}m_0)}{\partial x}+\frac{\partial(C_{gy}m_0)}{\partial y}+\frac{\partial(C_\theta m_\theta)}{\partial \theta}=T_0 \tag{9}$$

$$\frac{\partial(C_{gx}m_1)}{\partial x}+\frac{\partial(C_{gy}m_1)}{\partial y}+\frac{\partial(C_\theta m_1)}{\partial \theta}=T_1 \tag{10}$$

where $m_0(x,y,\theta)$ is zeroth moment of the action spectrum, $m_1(x,y,\theta)$ is first moment of the action spectrum. C_{gx} and C_{gy}, component in x and y direction, respectively of the group velocity, Cg. C_θ propagation speed representing the chance of action in the θ direction. x and y, Cartesian coordinate. θ is direction of wave propagation T_0 and T_1, source term. The moments $m_n(\theta)$ are defined as Eq. (11)

$$m_n(\theta)=\int_0^\infty \omega^n A(\omega,\theta)d\omega \tag{11}$$

where ω is the absolute frequency and A is the spectral wave action density.

The propagation speed C_{gx}, C_{gy} and C_θ are obtained using linear wave theory. These partial differential equations (Eqs. (9) and (10)) in the model are solved using Eulerian finite difference technique. The zeroth and first moment Eq. (11) of the action spectrum gives integral wave parameters.

Nearshore waves of an area depend on the offshore wave climate and its bathymetry. Hence a bathymetry of 50 *m* × 200 *m* resolution extending up to the offshore wave data point is prepared. In order to obtain nearshore wave characteristics of the study area, offshore wave heights and periods from different directions are allowed to propagate over the bathymetry. The model is executed independently for waves corresponding to ranges of wave heights and periods covering predominant wave approach angles that would propagate energy to the nearshore. The incoming wave energy is specified using constant values of the significant wave height (Hm0), mean wave period (Tm), mean wave direction (MWD), while the directional distribution is

also included by specifying the maximum deviation (directional spreading index, n = 16) from MWD. In order to provide adequate resolution to the wave field and stability criteria for the numerical scheme, suitable grid and directional spacing in X (50 *m*), Y (200 *m*) and θ (10) are selected. The upwind differencing scheme in θ direction is used while central differencing scheme is used in X-Y plane. To simulate the changes in wave conditions due to varying water depths resulting from tidal variations, a water surface elevation of 1.5 *m* above the chart datum corresponding to the high water is considered (Panigrahi and Misra, 2009). In catering for bottom dissipation, the wave friction coefficient is set to 0.002 (Nikuradase roughness parameter, Nikuradse, 1932). The wave breaking is enabled during model execution with constant $\gamma 1 = 1$, $\gamma 2 = 0.8$ and $\alpha = 1$. The parameter α controls the rate of energy dissipation after breaking, $\gamma 1$controls the wave steepness related breaking and $\gamma 2$ controls the amount of depth related breaking (Panigrahi et al., 2012). The results of selected nearshore wave transformation are presented in Fig. 3. The change in wave height from deep-water to shallow water (at 20 *m* depth) for selected wave directions are presented in Fig. 4. It is seen from the figures that the deep water combination of (Hs = 1.4 *m* and Tm = 7 *sec*.) remain mostly unchanged at 20 *m* water depth except for two incident directions SW and NE. Hence the same has been formed the basis for subsequent simulation of inner harbour wave penetration. Wave heights at various berths within the harbour basin are expected to be much lower than the above limits due to the planned protection afforded by the harbour layout.

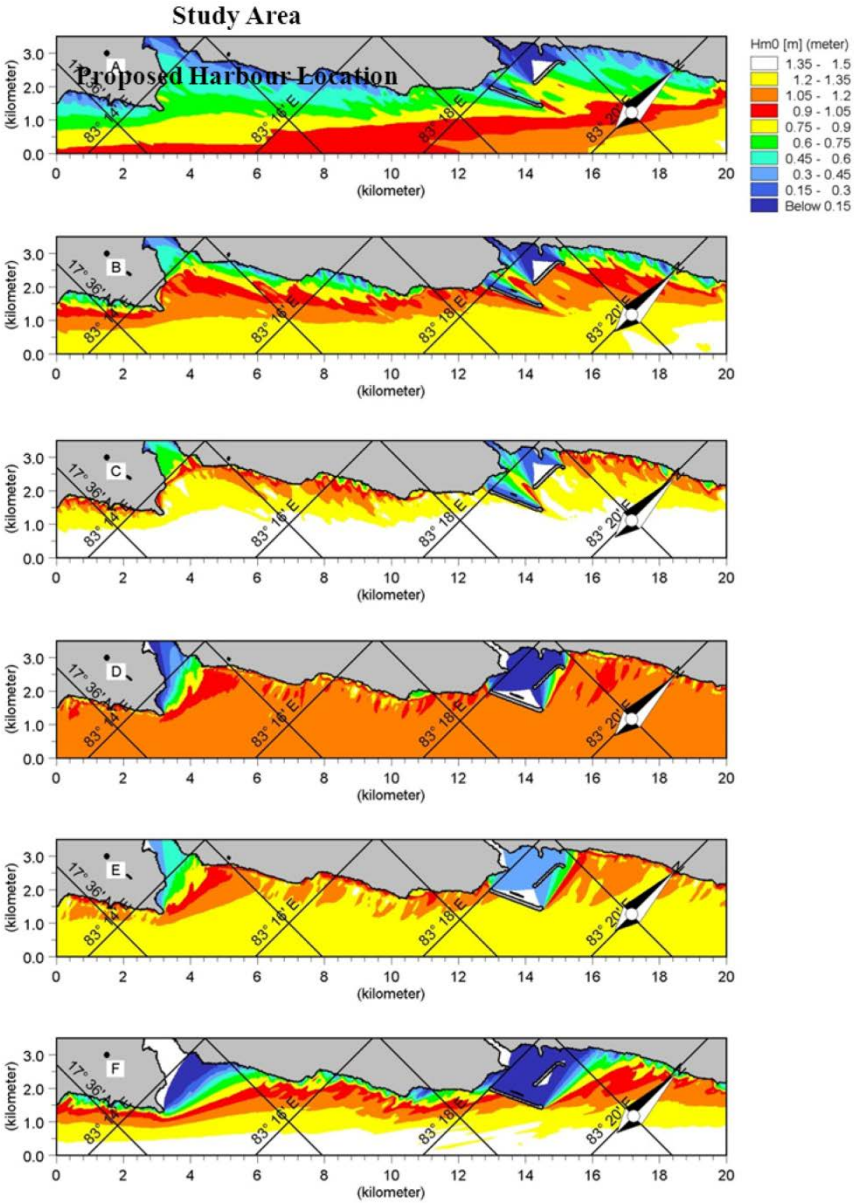

Fig. 3 Wave height contours for waves from (A) NE, (B) ENE, (C) E, (D) SSE, (E) S, (F) SSW directions.

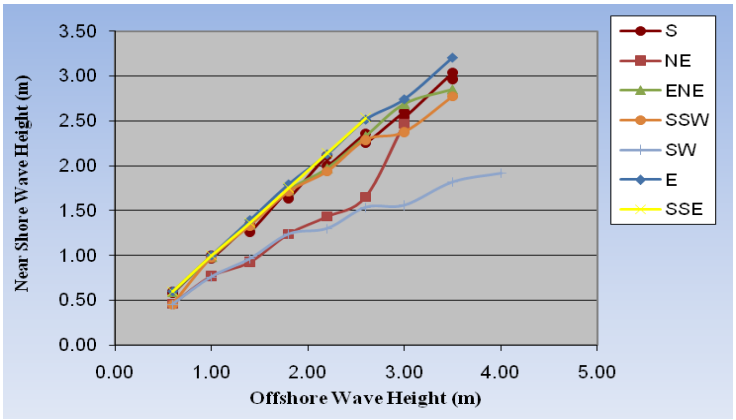

Fig. 4 Change in wave height from offshore to nearshore.

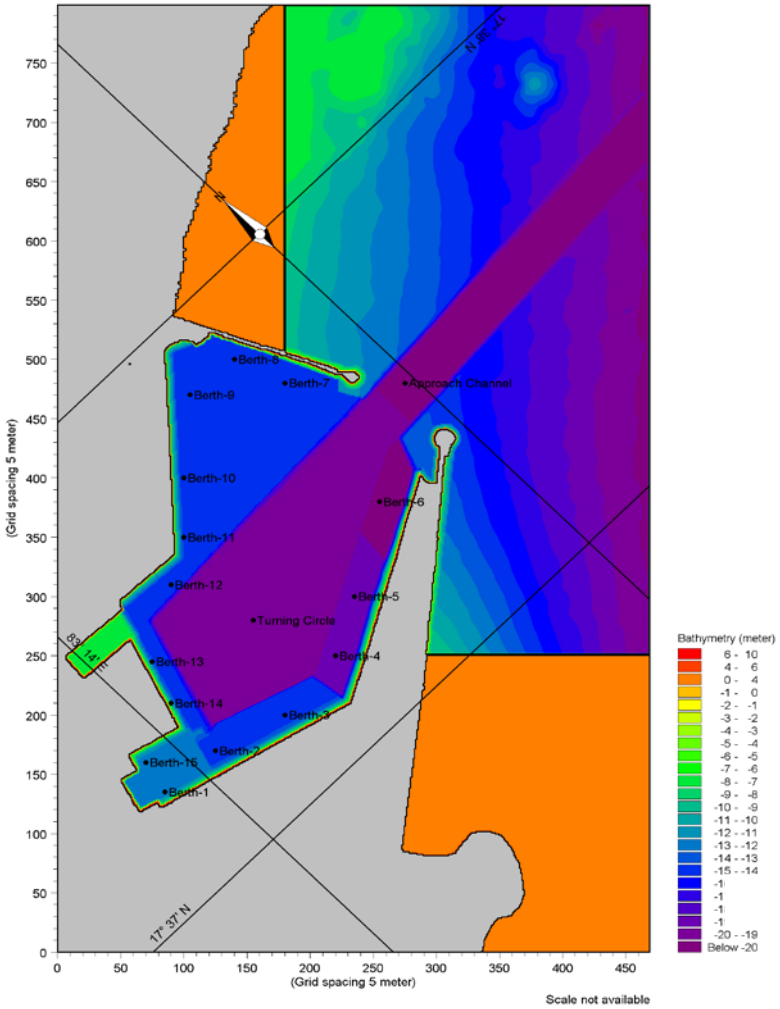

Fig. 5 Bathymetry and masterplan of the gangavaram port.

WAVE PENETRATION INTO HARBOUR

The Gangavaram port master plan is imposed on the bathymetry with a grid resolution of 5 *m* × 5 *m* for examining the inner harbor wave propagation. A model area covering approximately 4.5 *km* × 8 *km* including the approach channel, harbour break-waters, berths, dredged depths etc. are digitally laid to study the wave transmission into the harbour. The model area is rotated in such a way that the offshore boundary is parallel to the deep-water contours. The harbour layout is facilitated with 15 berths,

one approach channel and a turning circle, which are exactly scaled in the digital model as shown in the Figure Fig. 5. A critical threshold of Hs = 1.4 *m*, Tm = 7 *sec*. is chosen to be approaching from most probable directions NE, ENE, E, ESE, SE and SSE. A 30-minutes plot of irregular random wave (Hs = 1.4 *m*, Tm = 7 *sec*.) used as boundary conditions is presented in the Fig. 6. These waves from these predominant directions are allowed to approach in to the Gangavaram harbour using BW model of Mike21 (Madsen and Sørensen, 1992). The wave diffraction patterns within the area protected by the breakwater are analysed to assess the wave conditions at the locations of different berths within the harbour.

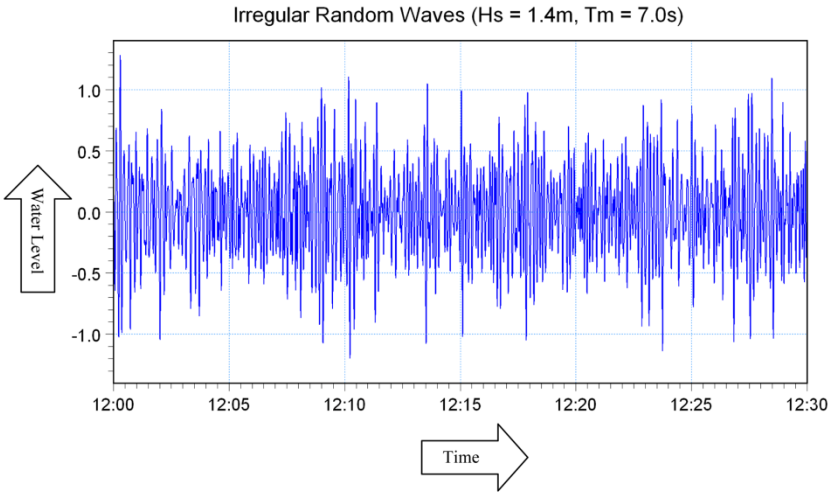

Fig. 6 Incident wave conditions at the harbour boundary.

The simulation experiment is conducted based on the time domain formulation by Madsen and Sorensen (Madsen and Sørensen, 1992). The Boussinesq Wave Model (BW, Mike21) solves the enhanced Boussinesq expressed in two horizontal dimensions (Abott et al., 2001) in terms of the free surface elevation, ξ and the depth-integrated velocity-components, along x-axis (P) i.e. (3) and y-axis (Q) i.e. (Eq. (14)). In this model, Boussinesq equations are solved by implicit finite difference techniques with variable defined on a space-staggered rectangular grid. The convective terms are discretised using central differrences and the normal ADI algorithm with 'side-feeding' is used for numerical integration. The 'side-feeding' technique (Abbott and Minns, 1998) is introduced to centre the cross-momentum derivatives without numerical dissipation.

The governing equations have the following form:

$$n\frac{\partial \xi}{\partial t}+\frac{\partial P}{\partial x}+\frac{\partial Q}{\partial y}=0 \tag{12}$$

X-momentum

$$\begin{aligned} &n\frac{\partial P}{\partial t}+\frac{\partial}{\partial x}\left(\frac{P^2}{h}\right)+\frac{\partial}{\partial y}\left(\frac{PQ}{h}\right)+\frac{\partial R_{xx}}{\partial x}+\frac{\partial R_{xy}}{\partial x}+ \\ &n^2 gh\frac{\partial \xi}{\partial x}+n^2 P\left[\alpha+\beta\frac{\sqrt{P^2+Q^2}}{h}\right]+\frac{gP\sqrt{P^2+Q^2}}{h^2 C^2}+n\psi_1=0 \end{aligned} \tag{13}$$

Y-momentum

$$\begin{aligned} &n\frac{\partial Q}{\partial t}+\frac{\partial}{\partial y}\left(\frac{Q^2}{h}\right)+\frac{\partial}{\partial x}\left(\frac{PQ}{h}\right)+\frac{\partial R_{xx}}{\partial x}+\frac{\partial R_{xy}}{\partial x}+ \\ &n^2 gh\frac{\partial \xi}{\partial y}+n^2 Q\left[\alpha+\beta\frac{\sqrt{P^2+Q^2}}{h}\right]+\frac{gQ\sqrt{P^2+Q^2}}{h^2 C^2}+n\psi_2=0 \end{aligned} \tag{14}$$

Where Boussinesq dispersion terms ψ_1 i.e. (5) and ψ_2 i.e. (6) are defined as

$$\psi_1 \equiv -\left(B+\frac{1}{3}\right)d^2\left(P_{xxt}+Q_{xyt}\right)-nBgd^3\left(\xi_{xxx}+\xi_{xyy}\right)$$

$$-dd_x\left(\frac{1}{3}P_{xt}+\frac{1}{6}Q_{yt}+nBgd\left(2\xi_{xx}+\xi_{yy}\right)\right)$$

$$-dd_y\left(\frac{1}{6}Q_{xt}+nBgd\xi_{xy}\right) \tag{15}$$

$$\psi_2 \equiv -\left(B+\frac{1}{3}\right)d^2\left(Q_{yyt}+P_{xyt}\right)-nBgd^3\left(\xi_{yyy}+\xi_{xxy}\right)$$

$$-dd_y\left(\frac{1}{3}Q_{yt}+\frac{1}{6}P_{xt}+nBgd\left(2\xi_{yy}+\xi_{xx}\right)\right)$$

$$-dd_x\left(\frac{1}{6}P_{yt}+nBgd\xi_{xy}\right) \tag{16}$$

where

P	Flux density in the x-direction, m3/m/s
Q	Flux density in the y-direction, m3/m/s
B	Boussinesq dispersion factor
X, Y	Cartesian co-ordinates
t	time in seconds
h	total water depth
d	Still water depth
g	Gravitational acceleration
n	porosity
C	Chezy resistance
α	Laminar flow resistance through porous media
α	Turbulent flow resistance through porous media and
ξ	water surface level above datum

The solutions to above flux based equations give various types of output results such as deterministic parameters, wave disturbance parameters and phase-averaged parameters.

The model capability and settings are described in this section. The short wave module of Mike-21 BW can model most wave processes like shoaling, refraction, partial reflection, diffraction, wave breaking, bottom dissipation, moving shoreline, wave transmission, non-linear wave-wave interaction, frequency and directional spreading. In order to reduce the computational points in simulations the bathymetry area outside north breakwater, close to the shore and those in southern portion outside the south breakwater are filled with artificial land points. The edges are decorated with sponge layers, such that wave energy reaching the shoreline and outside the harbour vicinity are absorbed in the areas of artificial land. This method is generally adopted in wave tranquility simulations; propagation of each wave train in these areas doesn't affect tranquility in the harbour

basin. Partial reflection from harbour breakwaters and berthing faces are also included in the simulations by specifying porosity values corresponding to reflection characteristics of the specified structures. The input irregular waves approaching harbour from critical directions are simulated using an in built facility in the model with $Cos^n(\theta-\theta_{main})$ directional spreading. These waves are allowed to propagate over the harbour breakwaters, into the inner harbour basin. Directional irregular waves confirming to the Pierson Moskowitz spectrum (Pierson and Moskowitz, 1964) with corresponding wave height, wave period and direction are used to define offshore wave conditions in simulations. Taking into account the maximum water depth, grid spacing and minimum wave period, the simulations are carried out using enhanced Boussinesq equations with a time step of 0.1 seconds. A surface elevation of 1.5 *m* above Chart Datum, corresponding to Mean High Water Spring (MHWS) is considered in all the simulations.

RESULT AND DISCUSSION

The WAM model hindcast offshore wave data are analysed and their directional distribution and occurrence frequencies are presented (Fig. 1). It is observed from the rose diagram that the offshore waves in the order of predominance from South (41.90%), SSE (13.88%), SSW (10.40%), ENE (7.94%), NE (4.53%), East (3.85%), ESE (1.20%) and SE (1.07%) directions reach to the nearshore. Fig. 1 shows that 84.77% of the total offshore wave climate is likely have influence the harbour tranquility. The exceedence probability analysis presented in Fig. 2 reveals that at deep-water, wave height exceeding 1.4 *m* (Hs) prevails approximately 52.17 days in a year. The same has been transformed to nearshore using nearshore spectral wave model and selected results are presented in Fig. 3. The change in wave height from offshore to 20 *m* depth is presented in Fig. 4 shows that waves from NE and SW suffers larger deviation from incident wave height and direction. Further, it is seen from the results of nearshore waves simulation that waves from SW-quadrant (S, SW, SSW) can largely be protected by orientation of southern breakwater. The critical wave characteristics would contribute to harbour tranquillity in normal operating condition is chosen to be (Hs = 1.4 *m*, Tm = 7.0 *sec*.) approaching from NE, ENE, E, ESE, SE and SSE respectively. The equivalent directional irregular wave group confirming to the Pierson Moskowitz spectrum is presented in Fig. 6. The majority of waves prevail inside the harbour are those incidents through the harbour entrance. The wave height in a harbour is in essence estimated as its ratio to the height of the incident waves at the offshore. The estimation has been done with due consideration of the random nature of sea waves, especially of the directional spreading of wave energy. As some wave energy may transmit to the interior of harbour by diffracting through structures, wave overtopping or passing through breakwaters. This complexity is expressed in a simplified form by taking a weighted mean of the wave energy for several directional components, on the basis of unidirectional estimated ratios of wave height, known as 'Wave Disturbance Coefficient'. The wave crest pattern and wave disturbance coefficients of resultant waves corresponding to the six critical directions (NE, ENE, E, ESE, SE and SSE) are presented in the Fig. 7 to Fig. 12 respectively.

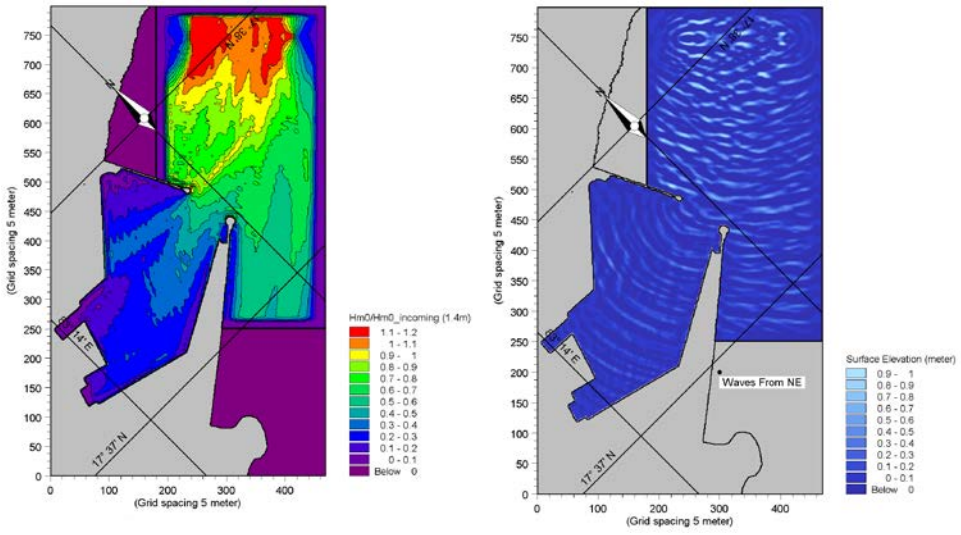

Fig. 7 Wave Disturbance coefficient & crest pattern for waves approaching from NE.

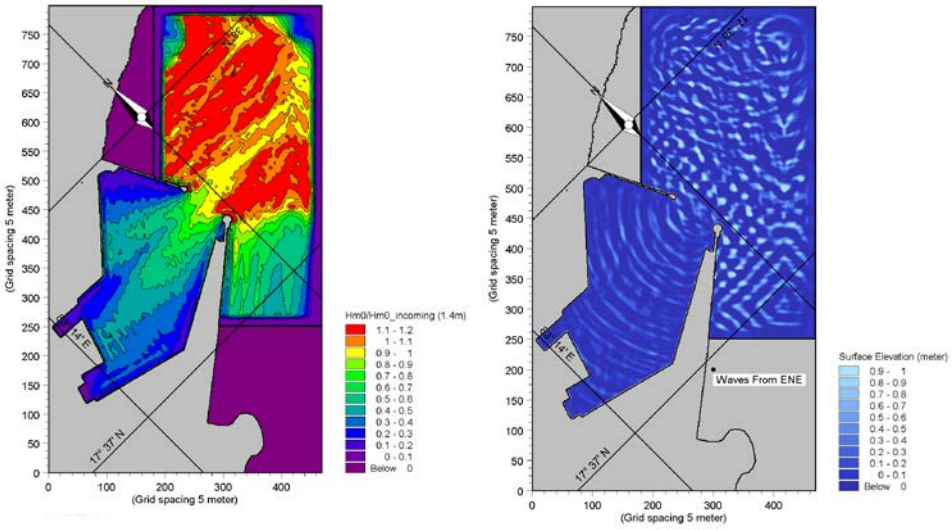

Fig. 8 Wave disturbance coefficient & crest pattern for waves approaching from ENE.

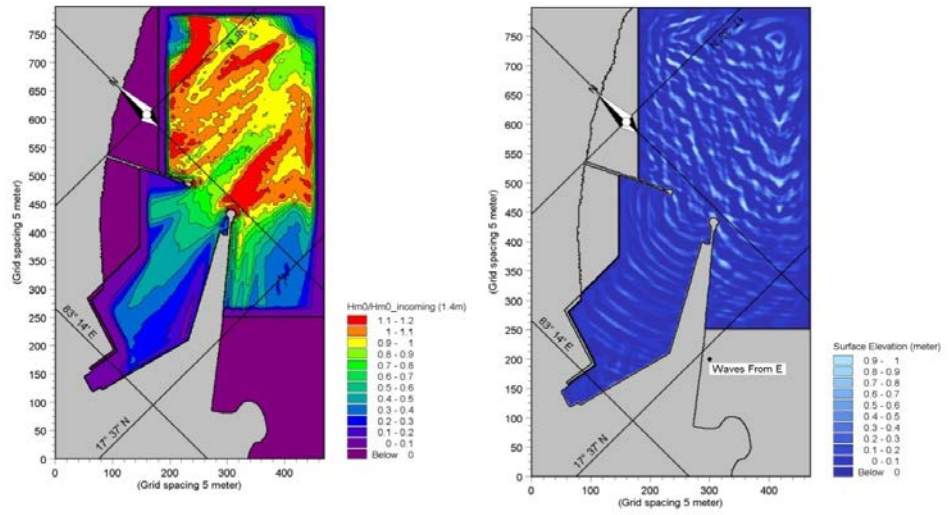

Fig. 9 Wave disturbance coefficient & crest pattern for waves approaching from E.

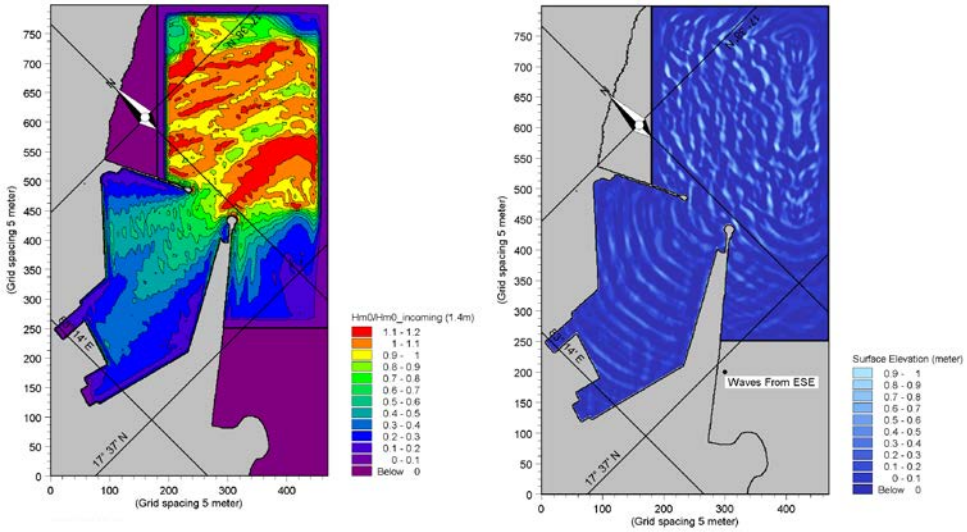

Fig. 10 Wave disturbance coefficient & crest pattern for waves approaching from ESE.

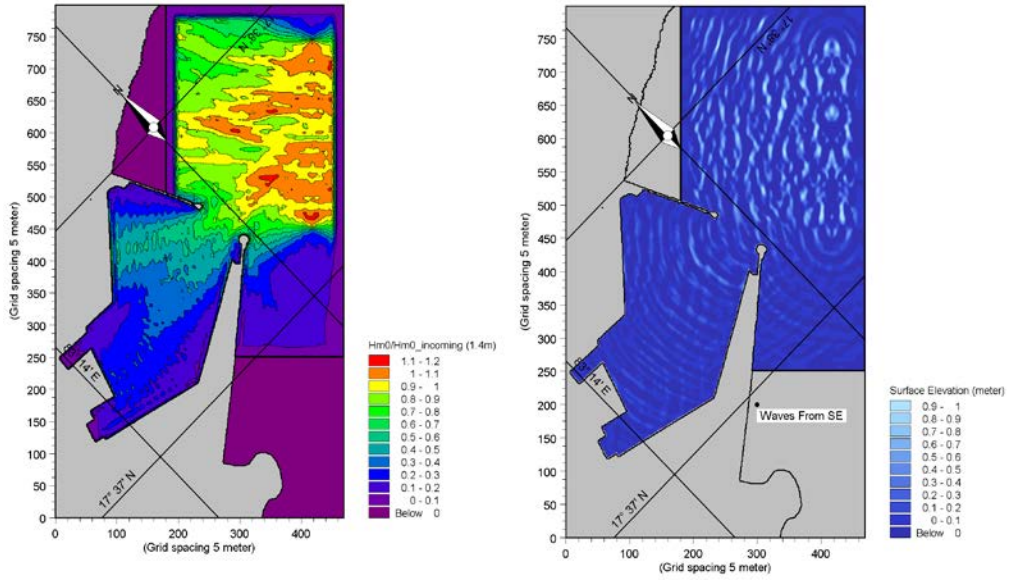

Fig. 11 Wave disturbance coefficient & crest pattern for waves approaching from SE.

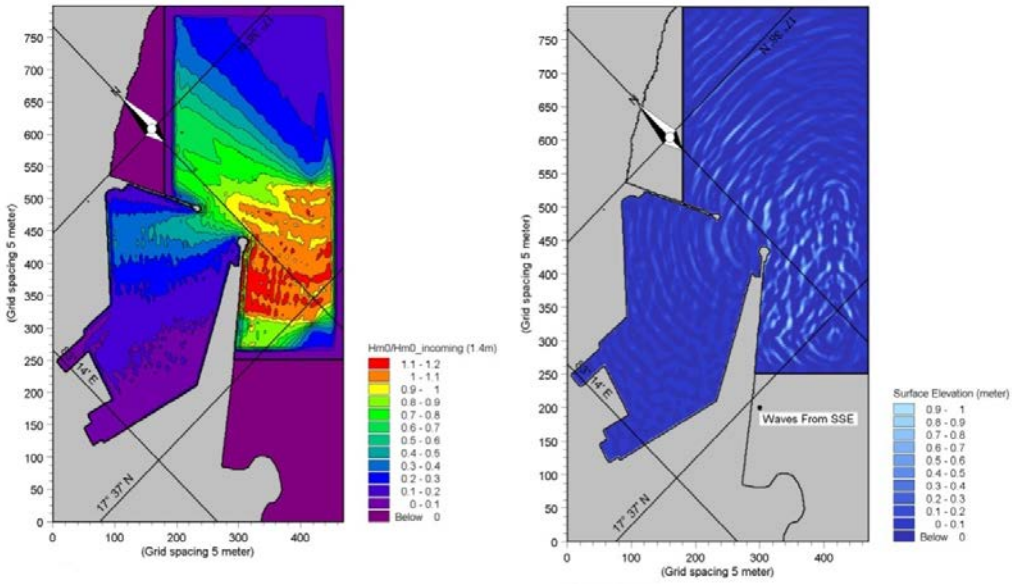

Fig. 12 Wave disturbance coefficient & crest pattern for waves approaching from SSE.

The wave crest pattern shows it's direction of approach and the diffraction at breakwaters, while the wave disturbance coefficient (%) shows tranquillity at various locations with respect to incoming wave heights. It is seen that, water depth is higher in the northern side of the harbour, around the location of general purpose (Berth no.10) and liquid berths (Berth no.7), which results in higher transmission of wave energy in to the harbour basin. The wave disturbance coefficients for resultant waves at various berths are presented in Table 1.

Maximum wave agitation levels predicted for the general purpose berths (Berth no.10 & 11) show wave disturbance coefficients are around 50% for waves from ENE and ESE. The two berths at the entrance harbour (Berth no. 9 & 6) have shown a wave disturbance coefficient in the order of 40%. Overall the results show that the harbour layout supresses most of the waves adequately except the waves approaching from ENE and ESE. These two directions are responsible for higher waves of the order 0.7 *m* at berths number 10 and 11, which is higher than the port operation limit of 0.5 *m* for handling cargos. Further a comparison of exceedence probability of wave heights at offshore, nearshore (at 20 *m* depth) and inner harbour (at turning circle) for most energetic wave approach direction is presented in Fig. 13. As mentioned earlier the tranquillity of a

harbour is evaluated with the safety of ships and the efficiency of cargo handling operations under constraints of construction and maintenance cost. In such evaluations, the amplitude of ship motions at mooring provides the most important information. Hence, time series plot for the complete simulation period (30 *minutes*), giving rise most energetic waves in the harbour is presented in the Fig. 14. The wave heights are below the prescribed thresholds for the mooring, berthing, line tending practices. Hence the inner harbour of Gangavaram is safe for normal operating wave conditions.

Table 1 Wave disturbance coefficient (%) at various berths for resultant waves (Hs = 1.4 *m*, Tm=7 *sec*.)

Direction	NE	ENE	E	ESE	SE	SSE
Berth-1	24	30	23	20	22	5
Berth-2	26	32	23	24	18	7
Berth-3	28	30	24	23	19	8
Berth-4	20	24	18	17	14	9
Berth-5	23	29	24	22	15	9
Berth-6	31	45	39	42	34	17
Berth-7	16	28	28	29	32	37
Berth-8	9	17	18	20	17	20
Berth-9	17	33	35	37	40	34
Berth-10	27	50	46	51	46	31
Berth-11	33	50	44	39	33	19
Berth-12	7	17	16	15	11	8
Berth-13	17	35	34	32	23	14
Berth-14	29	43	38	37	30	11
Berth-15	15	16	15	12	14	5
Turning Circle	26	44	37	35	30	10

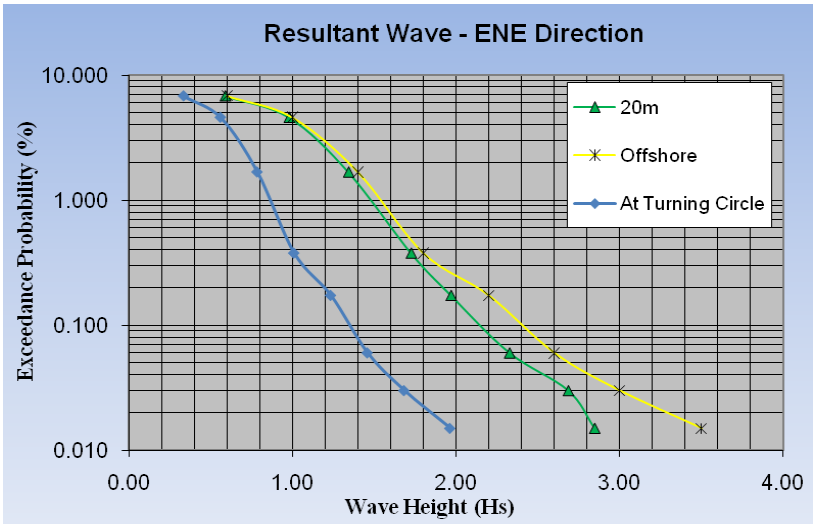

Fig. 13 Wave exceedence at offshore, nearshore and turning circle for energetic waves from NNE.

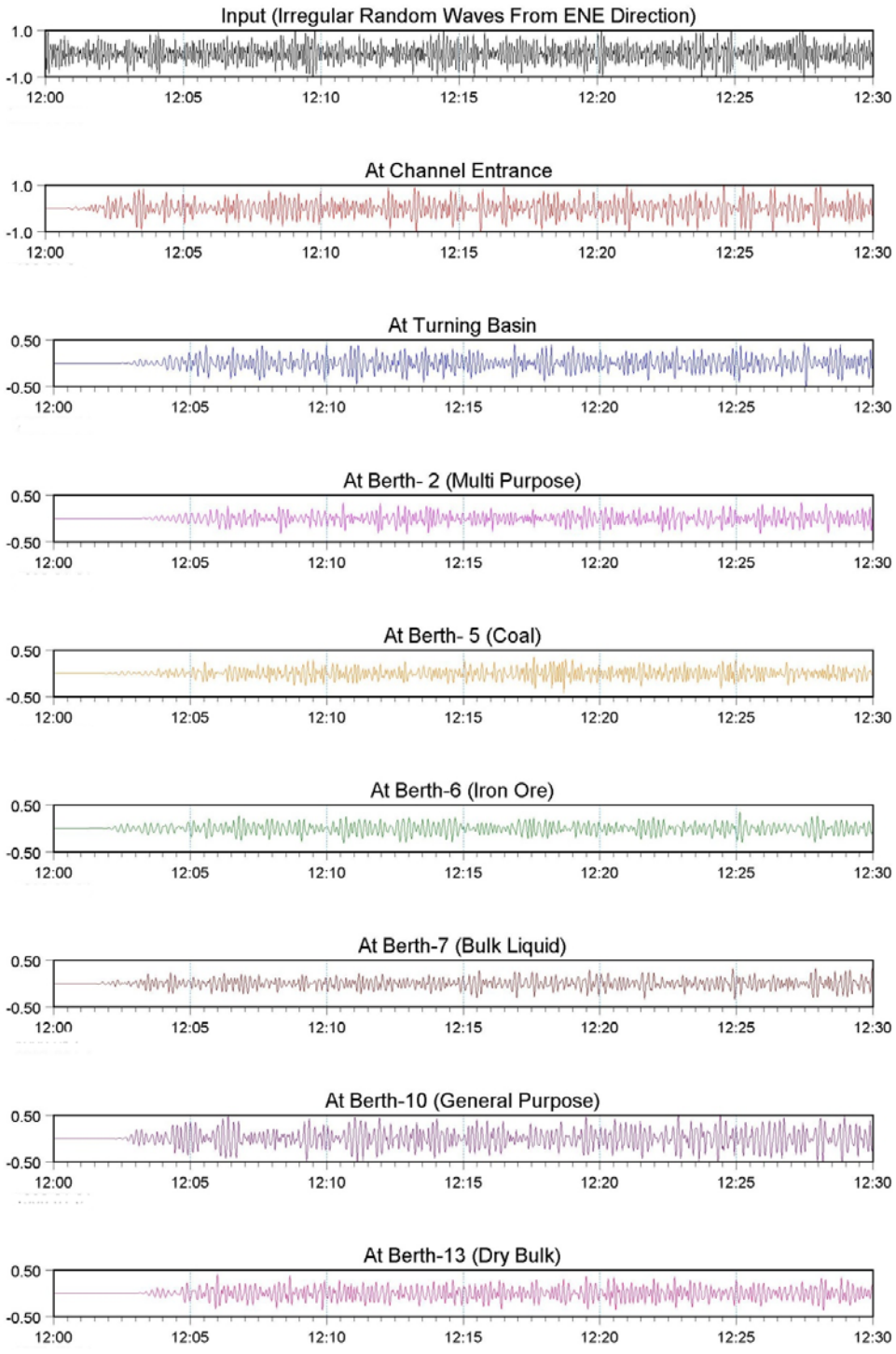

Fig. 14 Wave Agitation levels at selected berths.

CONCLUSION

Surface water waves have been modeled for an idealized test case demonstrating real practical applications in harbour planning. The deep water wave model WAM, Shallow water wave model NSW and Boussinesq wave model BW is well established models and validated during several studies by others (Zeki and Okey, 2007; Narayanaswamy et al., 2010). Simulation of offshore wave penetration to inner harbor is very essential for evaluating harbor tranquility. The simulated results of the model has provided keen insight into the performance of the harbour layout in the wave agitation point of view. The wave experienced at berth locations are of immense help to port planners for deciding the berth allocation as well as mooring

system for various types of vessels. The several principles for port planners and marine structure experts adopt to improve the harbour tranquillity are like, having a broad interior for a harbour, no wave reflection at the spot of first wave arrival, locating small-craft basin at a recess of a harbour, reservation of wave dissipation area along the waterfront, precaution to wave reflection from the back face of breakwater, caution on quay walls of the wave absorbing type etc (Goda, 2009). Although the tranquillity of a harbour cannot be completely characterised by means of wave height alone, this is an essence of harbour planning. Numerical techniques to obtain wave agitation inside the harbour are an efficient and economic approach compare to physical modeling.

ACKNOWLEDGEMENTS

This work is an offshoot of Ph.D. thesis of Dr. Jitendra K. Panigrahi, under the faculty of Marine Science, Berhampur University, India. The author is thankful to Berhampur University authorities for providing support and assistance for this work.

REFERENCES

Abott, M.B., Madsen, P.A. and Sorensen, O.R., 2001. *Scientific documentation of Mike21 BW- Boussinesq Wave Module*. MIKE by DHI.

Abbott, M.B., McCowan, A.D. and Warren, I.R., 1984. Accuracy of short-wave numerical models. *Journal of Hydraulics Engineering*, 110, pp.173-197.

Abbott, M.B. and Minns, A.W., 1998. *Computational hydraulics*. 2nd Ed. Aldershot: Ashgate Press.

Abbott, M.B., Petersen, H.M. and Skovgaard, O., 1978a. On the numerical modeling of short waves in shallow water. *Journal of Hydraulic Research*, 16(3), pp.173-203.

Abbott, M.B., Petersen, H.M. and Skovgaard, O., 1978b. Computation of short waves in shallow water. *Proceedings 16th international conference on Coastal Engineering, ASCE*, Hamburg, 1978, pp.414-433.

Airy, G.B., 1845. Tides and waves. *Encyclopaedia metropolitana. London*,192, pp.241-396.

Boussinesq, J., 1982. Theory of waves and swells propagated in a long horizontal rectangular canal, and imparting to the liquid contained in this canal approximately equal velocities from the surface to the bottom. *Journal de Mathematiques Pures et Appliquees*, 17(2), pp.55-108.

Boussinesq, J., 1877. Essai sur la theorie des eaux courantes. *Mem. divers Savants a L' Academie des Science*, 32, pp.56.

Goda, Y., 2009. Random seas and design of maritime structures. *Advanced series in ocean engineering*, 33, pp. 291-319.

Gunther, H., Hasselmann, S. and Janssen, P.A.E.M., 1992. *Wave model cycle 4'. Technical Report No*. 4. Hamburg: Max Plank Institute of Meteorology.

Holthhuijsen, L.H., 1998. A prediction model for stationary, short crested waves in shallow water with ambient currents. *Coastal Engineering*, 13, pp.23-54.

James, T.K., Ge, W., Qin, C., Andrew, B.K. and Robert, A.D., 1998. *Fully nonlinear boussinesq wave model documentation and user's manual, FUNWAVE 1.0, Centre for applied coastal research department of civil engineering, Research report No.CACR-98-06*. DE: University of Delaware.

Jeffreys, H. and Jeffreys, B., 2007. *Methods of mathematical physics*. 1rd. ed. Cambridge: Cambridge University Press.

Kamineni, R., Rizvi, S.R.H., Kar, S.C., Mohanty, U.C. and Paliwal, R.K., 2002. Assimilation of IRS-P4 (MSMR) meteorological data in the NCMRWF global data assimilation system. *Journal of Earth System Science*, 111, pp.351-364.

Komen, G.J., 1996. *Dynamics and modeling of ocean waves*. Cambridge: Cambridge University Press.

Kofoed-Hansen, H., Sloth, P., Sørensen, O.R. and Fuchs, J., 2003. Combined numerical and physical modelling of seiching in exposed new marina. *Proceedings of the 27th International Conference on Coastal Engineering*, Sydney, Australia, 2000, pp.3601-3614.

Korteweg, D.J. and De Vries, G., 1895. On the change of form of long waves advancing in a rectangular canal and on a new type of long stationary waves. *Philosophical Magazine*, 5(39), pp.422-443.

Kuang-ming, Y., Rugbjerg, M. and Kej, A., 1987. Numerical modelling of harbour disturbance in comparison with physical modelling and field measurements. *Proceedings of Second International Conference on Coastal and Port Engineering in Developing Countries*, Beijing, China, 1987, pp.165-171.

Lorenc, A.C., 1986. Analysis methods for numerical weatherprediction. *Quarterly Journal of the Royal Meteorological Society* , 112, pp.1177-1194.

Madsen, O.S. and Mei, C.C., 1969. *Dispersive long waves of finite amplitude over an uneven bottom, Report No.117*. Massachusetts: MIT, Hydrodynamic Laboratory.

Madsen, P.A., Murray, R. and Sorensen, O.R., 1991. A new form of the Boussinesq equations with improved linear dispersion characteristics, Part-1. *Coastal Engineering*, 15, pp.371-388.

Madsen, P.A. and Sørensen, O.R., 1992. A new form of the Boussinesq equations with improved linear dispersion characteristics. Part 2: A slowly-varying Bathymetry. *Coastal Engineering*, 18, pp.183-204.

Madsen, P.A., Sorensen, O.R. and Schaffer, H.A., 1997a. Surfzone dynamics simulated by a Boussinesq type model. Part-I, Model description and cross shore motion of regular waves. *Coastal Engineering*, 32, pp.255-288.

Madsen, P.A., Sorensen, O.R. and Schaffer, H.A., 1997b. Surfzone dynamics simulated by a Boussinesq type model. Part-II, Surf beat and swash zone oscillations for wave groups and irregular waves. *Coastal Engineering*, 32, pp.289-320.

Mei, C.C. and Le Mehaute, B., 1966. Note on the equations of long waves over an uneven bottom. *Journal of Geophysical Research*, 71(2), pp.393-400.

Narayanaswamy, M., Alejandro J C., Moncho G., R.A.Dalrymple., 2010. PHysics-FUNWAVE hybrid model for coastal wave propagation. *Journal of Hydraulic Research*, 48(Extra Issue), pp.85-93.

Nikuradse, J., 1932. Gesetzmassigkeiten der turbulenten Stroming in glatten Rohren. *VDA-Forschungsheft, Berlin*, 1932, pp.414-433.

Panigrahi, J.K., 2007. *Wind induced surface gravity waves in the north Indian Ocean and their potential applications*. PhD Thesis. Berhampur University, India.

Panigrahi, J.K. and Misra, S.K., 2009. Numerical hindcast of extreme waves. *Natural Hazard*, 53(2), pp.361-374.

Panigrahi, J.K. and Swain, J., 2010. Numerical simulation and validation of deep-water spectral wind-waves. *Marine Geodesy*, 33, pp.39-52.

Panigrahi, J.K., Umesh, P.A., Padhy, C.P., Swain, J., 2012. Nearshore propagation of cyclonic waves. *Natural Hazards*, 60 (2), pp.605-622.

Patrick, J.L. and Philip, L.F.L., 2004. *Modeling wave generation, evolution, and interaction with depth-integrated, dispersive wave equations, COULWAVE code manual*. New York: Cornell University.

Peregrine, D.H., 1967. Long waves on a beach. *Journal of Fluid Mechanics*, 27(4), pp.815-827.

Pierson, W.J. and Moskowitz, L., 1964. A proposed spectral form for fully developed wind seas based on the similarity theory of S. A. Kitaigorodskii. *Journal of Geophysical Research*, 69, pp.5181-5190.

Sørensen, O.R., Schäffer, H.A. and Madsen, P.A., 1998. Surf zone dynamics simulated by a Boussinesq type model. Part. III: Wave-induced horizontal nearshore circulations. *Coastal Engineering*, 33, pp.155-176.

Swain, J., 1997. *Simulation of wave climate for the Arabian sea and Bay of Bengal*. Ph.D. Thesis. Cochin University of Science and Technology, India.

Swain, J., Panigrahi, J.K., Vijayakumar, D. and Venkitachalam, N.R., 2003. Performance of 3G-WAM using IRS-P4 winds for its operational implementation in the Indian Ocean. *Proceedings of the Symposium on Microwave Remote Sensing Applications*, IIT, Mumbai, 21-23 January 2003, pp.21-23.

Ursell, F., 1953. The long wave paradox in the theory of gravity waves. Proceedings of Cambridge Philosophical Society, 49, pp.685.

WAMDI Group, 1988. The WAM model-a third generation ocean wave prediction model. *Journal of Physical Oceanography*, 18, pp.1775-1810.

Zeki, D. and Okey, G.N., 2007. *Boussinesq modeling of wave propagation and runup over fringing Coral Reefs, BOUSS-2D Model Evaluation Report ERDC, CHL*. Washington, D.C.: U.S. Army Crops of Engineers.